Cell free miRNAs are pharmacodynamic biomarkers for enhanced Dicer activity by Enoxacin in human patients with Amyotrophic lateral sclerosis

Iddo Magen[1,2], Hannah Marlene Kaneb[3], Maria Masnata[3], Nisha Pulimood[3], Anna Emde[1,2], Angela Genge[3], Eran Hornstein[1,2]

1 Department of Molecular Genetics, Weizmann Institute of Science

2 Department of Molecular Neuroscience, Weizmann Institute of Science

3 Montreal Neurological Institute-Hospital, McGill University, Montreal, Canada.

Correspondence for molecular research:

Eran Hornstein, Arnold R. Meyer Building, Room 313, Weizmann Institute of Science, Rehovot 76100, Israel, email: eran.hornstein@weizmann.ac.il

Correspondence for clinical research:

Angela Genge, Montreal Neurological Institute and Hospital, Department of Neurology, 3801 University Street, Suite 207, Montreal, QC, CA H3A 2B4, email: angela.genge@mcgill.ca

Running head: miRNAs as biomarkers for Enoxacin treatment in ALS

Number of words in abstract: 180

Number of words in main text: 5477 (excluding title page, abstract, references, figure legends and acknowledgments)

Number of figures: 7

Number of tables: 2

ABSTRACT

Background and Objectives: The activity of the RNAse III DICER is downregulated in sporadic and genetic forms of ALS. Accordingly, hundreds of miRNAs are broadly downregulated, and their mRNA targets are de-repressed. Enoxacin is a fluoroquinolone, which increases DICER activity and miRNA biogenesis. Here, we tested for the first time the molecular effect of Enoxacin on miRNA biogenesis in patients with ALS and demonstrated that Enoxacin engagement with DICER can be pharmacodynamically monitored, via miRNA levels in human patients.

Methods: In an investigator-initiated, first-in-patient study, REALS1, we explored miRNAs as pharmacodynamic biomarkers for Dicer activation. Thus, patients with sporadic ALS were dosed with oral Enoxacin twice daily for 30 days in a double blind, randomized clinical trial.

Results: The study demonstrated a global increase in cell-free miRNA levels in both plasma and CSF at all time points following Enoxacin treatment (400 mg or 800 mg/day), compared to baseline. Additionally, no serious adverse events were reported among patients.

Conclusion:

Enhancing DICER activity by Enoxacin, increases miRNA biogenesis in human patients with ALS. These results encourage testing Enoxacin efficacy in larger trials.

INTRODUCTION

Amyotrophic lateral sclerosis (ALS) is a devastating neurodegenerative syndrome of the human motor neuron system[1]. Other than Tofersen therapy for SOD1-ALS[2], disease-modifying treatments do not exist. Studies over the last 20 years have uncovered ALS-causing mutations in a number of genes[3], many of which encode for RNA-binding proteins (e.g. TDP-43, HNRNP A2/B1, HNRNP A1 and FUS). It is therefore hypothesized that dysregulation of RNA activity may be involved in the pathogenesis of ALS[4–8]. Accordingly, dysregulated splicing has been recently suggested to play an important role in pathogenesis because of the loss of normal TDP-43[9–12]. However, other facets of RNA dysregulation are not fully explored.

microRNAs (miRNAs) are endogenous non-protein-coding small RNAs. miRNAs silence messenger RNA (mRNA) expression by controlling translational inhibition and mRNA decay. The involvement of miRNAs in ALS pathogenesis is suggested by a global downregulation of miRNAs in motor neurons of patients with ALS[13–16].

DICER is an RNAse III, which works in concert with TDP-43 to promote miRNA biogenesis[17]. DICER cleaves the precursor miRNAs (pre-miRNAs), giving rise to single-stranded mature miRNAs[18]. The expression of ALS-causing mutant forms of TDP-43, FUS or SOD1, resulted in inhibition of DICER activity and accumulation of pre-miRNA species[13]. Consistently, spinal motor neuron-specific knockout of Dicer in adult mice resulted in progressive loss of motor neurons, denervation, and muscular atrophy[4].

While almost all miRNAs are dependent on DICER for biogenesis and function, miR-451a is Dicer-independent, as it is processed by Argonaute (Ago)[19]. Importantly, Dicer-dependent miRNAs compete with miR-451a in binding to the effector RNA induced silencing complex (RISC). Therefore, an increase in DICER activity results in relative upregulation of mature miRNAs and relative depletion of miR-451a[20].

Enoxacin is a fluoroquinolone, an antibiotic that was identified as an agonist of DICER complex activity, via increasing the binding of pre-miRNAs[21–23]. Enoxacin elevated miRNA levels in rat frontal cortex[24] and rescued expression of miRNAs that were downregulated by ALS-associated mutations in a cell line[13] or in iPSC-derived motor neurons[25]. This suggests that the general upregulation of miRNA levels can be beneficial by regulating key genes that modulate pathological phenotypes. Furthermore, Enoxacin mitigated some of the symptoms associated with motor deterioration in the SOD1G93A and TDP-43A315T ALS mouse models[13]. These preclinical data support the potential use of Enoxacin as a novel disease-modifying drug and prompted us to initiate a study of Enoxacin in patients with ALS.

Cell-free miRNAs are studied as potential biomarkers in neurodegeneration[25,27–58]. Accordingly, we have recently shown that circulating miR-181 can serve as an ALS prognostication biomarker in three patient cohorts [59,60] , that miRNAs can predict the response to Spinraza therapy in spinal muscular atrophy[61] and that miRNAs assist the diagnosis of frontotemporal dementia[62]. Therefore, we hypothesized that cell-free miRNAs might also serve pharmacodynamic analysis and could potentially reveal the engagement of Enoxacin onto its therapeutic target, DICER, in humans.

Here, we report the findings from a study of orally administered Enoxacin in patients with ALS. We found that Enoxacin globally increases miRNA levels in plasma and CSF and that the magnitude of the molecular changes in miRNAs is associated with the concentration of Enoxacin in plasma. Enoxacin was also safe and tolerable. Thus, our study provides means to quantify target engagement by DICER agonists and encourages further studies to assess the efficacy of Enoxacin in patients with ALS.

MATERIALS AND METHODS

Trial design and oversight

REALS1 (ClinicalTrials.gov identifier: NCT04840823) was a randomized, double-blind, parallel groups, phase 1b/2a study of Enoxacin in patients with ALS. Enoxacin was dosed orally at a 400mg, 800mg or 1200mg per day, which is the range used in humans, and the trial was limited to 30 days of dosing, as this period is known to be safe in humans[63, 64]. All enrolled patients were actively dosed and patient's baseline miRNA measurement, prior to initiation of therapy, was established on day 1 as a reference. No placebo group was included. The study protocol was approved by the Research Ethics Board at the Clinical Research Unit at The Neuro (Montreal Neurological Institute-Hospital (MNI, CRU / 2020-6359, Document S1)). The study enrolled participants at MNI, Montreal, Quebec, Canada from April 2021 through March 2023. All participants provided written informed consent, and experiments conformed to the principles set out in the World Medical Association (WMA) Declaration of Helsinki and the Department of Health and Human Services Belmont Report. Participants were evaluated and monitored in the clinic on days 1, 7, 14, 21, and 30 of treatment and at a follow-up visit 14 days after the last dose.

Sample size determination

This study was a small, early-phase study to assess dose range and design in preparation for a large-scale future efficacy trial. There was no effect size available for calculation at the time

the protocol was written. 36 patients (12 per treatment arm), were considered adequate for the initial assessment of safety, tolerability, PK, and PD of three doses of Enoxacin in adults with ALS. However, the number of recruited patients was dramatically affected by restrictions due to COVID and the burden the pandemic imposed, particularly on the participation of Canadian patients with ALS in a full 30-day study in Montreal Neurological Institute.

Participant inclusion criteria

Participants were diagnosed with either familial or sporadic ALS and were on a stable dose of Riluzole for at least 30 days prior to screening. Participants with a forced vital capacity (FVC) lower than 50% of what is expected by age, height, weight, and sex were excluded. reported hypersensitivity/allergy to fluoroquinolone was an exclusion criterion. Diagnosis of an additional neurodegenerative disease, pulmonary disorder not attributed to ALS, severe renal impairment or impaired liver function also resulted in exclusion. Patients currently enrolled in another clinical trial involving an experimental drug or device were excluded as well.

Randomization and blinding

Patients were randomly allocated to one of the dosing groups and were administered with a single morning dose and a single evening dose of Enoxacin for 30 days (Figures 1, 2). A single morning dose (200mg, 400mg or 600mg) was administered on days 1 and 30 to determine Enoxacin pharmacokinetics (Cmax, Tmax) over 24 hours. The study statistician generated a random allocation sequence, enrolled participants, and randomly assigned them to interventions as per the sequence. Block randomization with block size of 3 was used to achieve balance and maintain the blind. The study statistician and a delegated individual not involved in the day to day running of the study were unblinded to the randomization code for the purposes of the generation and verification of this code, however they had no contact with study participants and were unaware of the identity of the study participants, whose treatment were assigned based on this allocation sequence.

The sponsor, study participants, principal investigators, coordinators, clinical laboratory staff and all other study site staff except for the study pharmacist(s), were blinded to participant treatment dose assignment throughout the study. To preserve blinding, an identical placebo tablet composed of excipient only was provided to patients assigned to doses that did not require 3 ‘active’ 200mg Enoxacin tablets to complete one dose. Thus, patients receiving 200mg Enoxacin x 2 / day took one 200mg Enoxacin tablet and two placebo tablets twice daily, patients receiving 400mg x 2/day took two 200mg Enoxacin tablets and one placebo tablet twice daily, and patients receiving 600mg x2/day took three Enoxacin tablets twice daily.

Enoxacin and placebo tablets were in-kind gifts from Apotex, Inc., Toronto, Canada.

Study endpoints

We sought unbiased analysis of miRNA levels in the plasma on days 1, 7, 14, 21 and 30 and in the CSF on days 1 and 28. To allow for pharmacokinetic-pharmacodynamic relationship, pharmacokinetic analysis of Enoxacin levels was done in plasma on days 1, 7, 14, 21 and 30.

Safety and tolerability of Enoxacin included the following assessments: adverse events (AEs), including AEs related to the drug, and serious AEs, i.e. AEs that affect patient's safety and require medical intervention. Adverse events (AEs) were coded to preferred terms from the MedDRA library (version 23.0). Additional safety assessments included physical examination; body weight; 12-lead electrocardiogram (ECG) parameters; vital signs; laboratory safety assessments; and FVC predicted percentage. The tolerability of Enoxacin was determined based on rates of AEs and the discontinuation of the study drug due to drug-related AEs. An illustration of the study design and its endpoints is seen in Figure 2. Secondary outcomes included Amyotrophic Lateral Sclerosis Functional Rating Scale-Revised (ALSFRS-R) score at baseline and at the end of the follow-up period on day 30 and pharmacokinetic analysis of Riluzole on days 1 and 30.

Biofluid collection

Phlebotomies were performed before Enoxacin morning dosing on days 1, 7 (+/- two days), 14 (+/- two days), 21 (+/- two days) and 30. After blood withdrawal, cells were pelleted by centrifugation at 2000 RPM for 10 minutes at 4°C. The plasma was transferred to a separate tube and stored at -80°C. Cerebrospinal fluid (CSF) was collected by lumbar puncture (LP) before dosing on day 1, and two hours (+/-one hour) post dosing on day 28. CSF samples were centrifuged at 2000 RPM for 10 minutes at 4°C to pellet cells. LP was performed only for participants who specifically consented to this procedure.

Pharmacokinetic analysis

Trough plasma concentrations of Enoxacin (ng/ml) were measured before administration of the morning dose on days 1 (before treatment onset), 7, 14, 21, and 30 to determine steady-state levels. Plasma concentrations were also measured 1, 2, 4, 6, 8, and 24 hours after dosing on days 1 and 30 to determine C_{max} (maximal concentration) and t_{max} (time to reach maximal concentration) after a single dose of Enoxacin. Enoxacin concentrations were measured by liquid chromatography with tandem mass spectrometry (LC-MS/MS) at SGS Life Science Services (Saint-Benoît, France). Plasma concentrations of Riluzole (ng/ml) were measured 2,

4, 6 and 8 hours after Enoxacin dosing on days 1 and 30 to determine potential inhibitory effect of Enoxacin on Riluzole metabolism, as reported previously[65]. Riluzole was measured by Protein-precipitation extraction / HPLC with MS/MS at Aliri Bioanalysis (Salt Lake City, Utah).

Biomarker assays

miRNA profiling. Total RNA was extracted from 0.5-1 ml of plasma or CSF using the miRNeasy micro kit (Qiagen, Hilden, Germany) by an experimenter blinded to the identity of samples. Repeated samples from the same individuals were processed in the same batch to avoid confounding effects of batch-to-batch variation on differences between repeated samples. Small RNA-seq libraries were prepared from 5µl total RNA using the QIAseq miRNA UDI Library Kit and QIAseq miRNA 96 Index Kit IL UDI-A (Qiagen) in a blinded fashion, keeping the same batches as library preparation. 3' and 5' adapter ligation was followed by reverse transcription. Precise linear quantification of miRNA was achieved by 12-nucleotide long unique molecular identifiers (UMIs) within the reverse transcription primers[66]. cDNA libraries were amplified by 22 cycles (plasma) or 23 cycles (CSF) of PCR, with two unique dual indices (UDIs) of 10 nucleotides, followed by on-bead size selection and cleaning. Library concentration was determined with a Qubit fluorometer (dsDNA high sensitivity assay kit; Thermo Fisher Scientific, Waltham, MA) and library size with Tapestation D1000 (Agilent). Libraries with different indices were multiplexed and sequenced on Novaseq 6000 S1 flow cell (Illumina), with 72-bp single read and 10-bp read for index 1 and index 2. Fastq files were de-multiplexed and human miRNAs were mapped using miRBase[67] reference and the RNA-seq Analysis & Biomarker Discovery Portal (GeneGlobe, Qiagen).

Neurofilament analysis. NFL concentrations were measured in duplicates by a single molecule array (Simoa, Quanterix, Boston, MA, USA), using a bead-conjugated immunocomplex and NF-light Advantage Kit for HD-1/HD-X adjusted for SR-X (Uman Diagnostics Umea, Sweden). The immunocomplex was applied to a multi-well array designed to enable imaging of every single bead. A calibration curve constructed using serially diluted bovine NFL standard (UmanDiagnostics) enabled precise quantification of the average number of enzymes per bead per sample of plasma or CSF (diluted 1:4 and 1:100, respectively). The experimenter was blinded to labels and analysis comprised a single batch of reagents.

Statistical analysis

After alignment of sequencing reads to the human genome, only miRNAs with UMI counts >50 in at least 50% of plasma samples, or an average UMI count >20 across all samples in the

CSF were included in the analysis. To reduce subject-to-subject variability, counts were batch-corrected using the ComBat function, whereby each subject is considered a batch, as in our previous works[60–62]. Batch-corrected counts were further divided, either by the corresponding levels of miR-451a, a dicer-independent miRNA[19] to create a “DICER score” that takes into account two opposing effects of dicer enhancement; or by a size factor generated by the DESeq2 algorithm which takes into account library size geometric mean[68], under the assumption that miRNA counts followed a negative binomial distribution. Total miRNA abundance was calculated by summing the abundances of all miRNAs (whether divided by miR-451a or normalized by DESeq2).

Principal Component Analysis (PCA) was employed to reduce dataset dimensionality and to identify data patterns that correspond to the largest variances. Data were standardized to have a mean of zero and a standard deviation of one, ensuring that all variables contributed equally to the analysis and then eigenvalues and eigenvectors of the covariance matrix were calculated to determine the principal components. A transformation into a new coordinate system facilitated the visualization of only the two principal components with the largest variances being presented.

K-mean clustering was performed using R. Multiple miRNA expression was partitioned into predefined distinct non-overlapping clusters by minimizing the sum of distances between the data points and their respective cluster centroids. Data points consisted of each miRNA’s mean abundance and fold change post-treatment vs baseline. Data were first normalized to prevent scale dependencies that could bias the distance calculations. Based on preliminary analysis data were divided into k=2 distinct clusters. Plasma NfL levels following treatment were analyzed with one-way repeated measures ANOVA. Plasma abundance of multiple miRNA species following treatment was analyzed by repeated measures two-way ANOVA wherein time point was included as a repeated factor and miRNA species as an additional factor. Pairwise comparisons were performed between post-treatment points (days 7, 14, 21 and 30) and baseline.

Comparison of plasma abundance of multiple miRNAs averaged over days 7, 14, 21 and 30 to baseline abundance, as well as of CSF abundance of multiple miRNAs post-treatment to baseline, was performed with paired t-tests for the different miRNA species, followed by correction to multiple hypotheses.

Post-treatment plasma total miRNA abundance was analyzed with a non-parametric Friedman test, followed by pairwise time point comparisons (post-treatment vs. baseline). The

significance of averaged plasma total miRNA abundance (days 7, 14, 21 and 30 averaged), as well as CSF total miRNA abundance and NfL (post-treatment vs. baseline), were determined with paired t-tests. Number of increasing vs decreasing miRNAs following Enoxacin was compared with the one-sample sign test, under the null hypothesis that half of the miRNAs increase and half of them decrease. Average fold change across all miRNAs was compared to a theoretical mean of 1 using the one-sample t-test.

In the case of multiple hypotheses testing (i.e. multiple time points tested vs baseline or multiple miRNAs tested between time points), p-values were corrected according to Benjamini and Hochberg[69], or the two-stage linear step-up procedure of Benjamini, Krieger, and Yekutieli[70]. The false discovery rate (FDR) was set at 0.1. Statistical analyses were performed with R (version 4.2.0, R Foundation for Statistical Computing, Vienna, Austria) or GraphPad Prism version 10.2.3 (GraphPad Software, Boston, Massachusetts USA). Graphs were generated using GraphPad Prism version 10.2.3.

RESULTS

Enoxacin elevates cell-free miRNA levels in the plasma, demonstrating enhancement of Dicer activity

A total of 13 patients living with ALS were screened for the study, of whom 8 passed included and enrolled (Figure 1). Recruitment occurred between April 2021 and March 2023, and the last patient follow up was in April 2023. Participants' baseline characteristics are presented in Table 1. One patient in the 600mg x2/day group dropped out early from the study (see below), leaving only n=1 patient in this group who completed the dosing period. We therefore performed in-depth analysis of data associated with the other two doses. Due to the small number of observations in the 200mg x2/day and 400mg x2/day groups (n=3 per dose), samples from the six patients were analyzed together. Enoxacin is an agonist of the Dicer complex[21,23,25] and is expected to upregulate miRNA biogenesis in tissues[13]. We hypothesized that Enoxacin would elevate the levels of many miRNAs and that accordingly next-generation sequencing of cell-free miRNAs could serve as a pharmacodynamic (PD) marker of target (DICER) engagement. Plasma samples were collected by phlebotomy at baseline before treatment initiation, and on days 7, 14, 21, and 30 before the morning dose. Small RNA libraries were prepared and sequenced on the Illumina NovaSeq platform with a 72-bp single read, followed by mapping of gained sequences into the human genome. As many as 2632 individual miRNA species were aligned to the human genome (GRCh37/hg19) across all samples. We included in the downstream analysis only miRNAs with UMI counts >50 in at least 50% of plasma samples (N=92 miRNAs). The repeated sampling from subjects allowed us to estimate the mean shift in read counts associated with each subject. We adjusted the original counts using the mean shift to reduce the confounding effect of subject-to-subject variability. We analyzed the difference in abundance of miRNAs between post-treatment time points and pre-treatment baseline. Because miR-451a is a DICER independent miRNA[19], which competes with dozens of DICER-dependent miRNAs on binding Argonaute proteins in the miRNA effector complex[20], the enhancement of DICER activity results in upregulation of all miRNAs other than miR-451a that is downregulated. Accordingly, we devised a DICER score that displays the ratio of all miRNA counts, divided by the sample levels of miR-451a.

Of the 92 miRNAs included in the analysis, 31/92, 35/92, 43/92, 32/92 increased significantly in their DICER scores on days 7, 14, 21, and 30 respectively (Figure 3A-D) and 59 miRNAs increased significantly when DICER score was averaged on measurements performed under therapy (Figure 3E). Importantly, no miRNAs decreased in a significant manner at either time point compared to baseline. Furthermore, the average DICER score of 89 out of 92 miRNAs

increased relative to baseline (97% of miRNAs, one-sample sign test: $Z=9$, $p<0.0001$). The mean effect size was a 2.5-fold increase in the DICER score (one-sample t-test, $p<0.0001$). These results demonstrate that Enoxacin increases miRNA levels in human patients with ALS.

In order to reduce the dimensionality of the dataset, which is composed of multiple miRNAs, we ran principal component analysis (PCA) on the DICER scores averaged on measurements performed under therapy, (days 7, 14, 21 and 30) relative to the baseline DICER scores (Figure 3F). Baseline samples and post-treatment samples were well-separated. Since the post-treatment samples are better clustered than baseline samples, Enoxacin reduces variability in DICER scores, and this might be due to enhancing dicer activity to the maximum.

Notable miRNAs that increased at all time points are the miR-320 family members (miR-320a, miR-320b, miR-320c, and miR-320d), the muscle-enriched miR-206 and miR-378a and the blood enriched miR-486-5p. We next grouped the 92 miRNAs into distinct groups, based on similar mean abundance and fold change. This step simplifies data interpretation and highlights miRNAs that consistently behave similarly under the effect of Enoxacin. Specifically, miR-16, miR-423, and miR-486-5p clustered together, in combination with let-7b/a (Figure 4) and may serve as potential biomarkers set for the molecular response to Enoxacin.

We also compared the total abundance of miRNAs on days 7, 14, 21, and 30 and at all post-treatment time points averaged, to baseline. Total DICER score was calculated by summing the DICER scores of all individual miRNAs. There was an overall increase in total DICER score when each post-treatment time point was compared to the baseline (Friedman test: $p<0.01$, Figure 5A). The highest increases in total DICER scores were observed on days 14 and 21: 3.4-fold and 3.1-fold, respectively, from 170±45 at baseline to 583±381 on day 14, and 526±226 on day 21 (q value = 0.007 and 0.004, respectively, after multiple hypothesis correction). In addition, the total DICER score at all post-treatment time points averaged was 2.5-fold higher than baseline (422±17.5 vs 170±45, paired t-test: $p<0.0001$, Figure 5B). When total miRNA abundance was calculated by summing the miRNA levels normalized by DESeq2, the average abundance across all post-treatment time points increased relative to baseline (paired t-test: $p=0.042$, Supp. Figure 1).

Taken together, Enoxacin elevates miRNA levels in plasma at all time points compared to baseline; miR-451a levels are reduced, and a robust effect is monitored when we consider a DICER score that divides levels of all miRNAs by miR-451a levels. The data suggest target engagement of Enoxacin with Dicer in humans and corroborates pre-clinical works measuring miRNAs in animal tissues.

Enoxacin elevates miRNA levels in the CSF

We next studied miRNA abundance in the CSF in samples collected from patients who specifically consented to this procedure (n=4). CSF reflects the cerebral microenvironment and thus can be a better approximation of the Enoxacin effect in the brain. Similar to plasma, miR-451a significantly decreased by 40%, from 14.8±1.8 UMIs at baseline to 8.85±1.6 UMIs post-treatment (Figure 6A, paired t-test: p=0.04). We then divided all miRNA levels by miR-451a to create a DICER score, as was done in plasma. Total DICER score in the CSF significantly increased by 70%, from 731±37 at baseline to 1259±86 post-treatment (Figure 6B, paired t-test: p=0.018).

We further focused on 24 miRNAs that increased in plasma at all time points (source data table 1) and were also detected in the CSF (average UMI count >20 across all samples). Eight out of these 24 miRNAs were significantly elevated in the CSF: four members of the miR-320 family (miR-320a-d), let-7c, miR-2110, miR-378a and miR-423 (Figure 6C, adj. p value < 0.05). miR-378a increased by 3.4-fold, compared to baseline.

We also measured NfL. Within the short period of therapy, NfL levels were not expected to change in the plasma or CSF and we did not reveal any significant differences at any time point relative to baseline (Supp. Figure 2).

Pharmacokinetic study of Enoxacin and Riluzole

We quantified the average Enoxacin plasma concentrations (before the morning dose, Supplementary table 1) and revealed that the average C_{max} was reached within two hours of administration. Enoxacin trough concentrations were rather constant from day 7 until the end of drug dosing on day 30. Therefore, Enoxacin levels were at a steady state at the time points in which pharmacodynamic markers were measured.

The concentrations of Riluzole, a common therapy for patients with ALS, were measured at 2h, 4h, 6h and 8h after Enoxacin administration on days 1 and 30. Higher Riluzole concentrations on day 30 (Supplementary table 2), suggests an Enoxacin-Riluzole interaction, in agreement with reported in vitro effects[65]. However, measured Riluzole levels did not exceed the C_{max} reported to be safe, given a dose of 50mg BID twice daily[71,72]. This suggests Riluzole levels are within the safe range, in agreement with lack of Riluzole-related adverse events.

Pharmacokinetic-pharmacodynamic relationship

To study the association between plasma trough Enoxacin concentrations and miRNAs, we performed pharmacokinetics-pharmacodynamic (PK-PD) analysis. At least 13 miRNAs were

significantly correlated with Enoxacin concentrations on day 14 (Figure 7), where the maximal effect of Enoxacin on total miRNA abundance was observed (Figure 3B). One data point was omitted due to a technical failure in measuring Enoxacin. The miRNAs were upregulated at least 2.5 fold and displayed Pearson correlations ≥ 0.89 (FDR<0.1). The association between Enoxacin levels and miRNA abundance supports the interpretation that Enoxacin enhances miRNA biogenesis.

Safety and tolerability of Enoxacin in people living with ALS

All participants experienced adverse events (AEs; Supplementary table 3), but most of the AEs reported were mild (36/52 events, 69%) or moderate (13/52, 25%). Severe AEs (3/52, 6%) were not life-threatening, or serious (0/52). The three severe AEs were as follows: deep vein thrombosis in one patient (dosed at 200mg x 2/day), probably not related to Enoxacin and resolved after increasing the dose of an anticoagulant, apixaban, which the patient has been taking regularly for at least six years. Nausea in another patient (dosed at 200mg x 2/day), was resolved after taking dimenhydrinate (Dramamine). Dizziness in a third patient (dosed at 400mg x 2/day), decreased in severity during the next visit without medical intervention.

One patient in the 600mg x 2/day dosing group, which was excluded from analysis (see methods) experienced mild or moderate nausea and dizziness that were assessed as related to Enoxacin. These were defined as (Supplementary table 3), were not life threatening, but were symptomatically severe enough to cause early discontinuation of Enoxacin before completion of the dosing period.

AEs related to Enoxacin did not cause an early drop-out in any other patient and all participants completed the dosing period and did not miss any dose of Enoxacin, with the exception of a single patient that was treated with the highest dose of 600mg x 2/day. In addition, throughout the dosing period none of the patients presented significant abnormalities in ECG, vital signs (blood pressure and pulse rate), or blood tests. All the AEs seen were previously observed in the original development of Enoxacin for antimicrobial indications. In addition, although potential interaction of Enoxacin with Riluzole was suggested in vitro[65], none of the AEs were deemed related to a possible change in Riluzole levels.

Taken together, enhancing DICER activity by Enoxacin increases miRNA biogenesis in human patients with ALS, without any safety concerns.

DISCUSSION

In our study, we measured miRNAs as biomarkers and molecular endpoints for the effects of Enoxacin. Because of the known effect of Enoxacin on DICER and its substrate, miRNAs, we profiled miRNAs as pharmacodynamic and target engagement biomarkers. Most of the miRNAs were increased as a result of Enoxacin treatment in both plasma and CSF, supporting the engagement of Enoxacin with its target. The extent of the effect of Enoxacin on miRNAs. i.e. the increase in their levels was correlated with the concentration of Enoxacin in the plasma, which further supports target engagement.

A main question of our study was whether Enoxacin could have an effect in the CSF, a potential reflection of the central nervous system as the target tissue. Previous works show that the ratio of CSF to plasma levels is 33.3% in dogs[73], and 20% in rats[74,75], suggesting substantial penetration of Enoxacin into the CSF from the blood. One study found a ratio of 29% in the CSF and 10% in the brains of rats[76]. In agreement with these studies, we observed an effect of Enoxacin on miRNA levels in the CSF, and three of the miRNAs that were increased in the CSF - let-7c, miR-16 and miR-320a - are abundant in both the human brain and spinal cord (>1000 copies)[77]. Together, the findings suggest that Enoxacin can affect miRNA biogenesis within the central nervous system when administered orally.

Some of the miRNAs that were increased by Enoxacin treatment were reported to be neuroprotective, in the context of ALS or brain injuries. For instance, miR-139 was downregulated in postmortem motor neurons of ALS patients by 8-fold[15], and in ALS iPSC-derived motor neurons, leading to upregulation of the Wnt/β-catenin pathway which is a driver of motor neuron degeneration[78]. Thus, restoring miR-139 levels in ALS may be beneficial to motor neurons by regulating the Wnt/β-catenin pathway. Other miRNA that were increased by Enoxacin were miR-130a, which displays neuroprotective activity after cerebral ischemia upstream of the PTEN/PI3K/AKT pathway[79–81], Let-7c, miR-378a, miR-486 and miR-93 that were reported to regulate microglial activation, suppress neuroinflammation and inhibit neuronal apoptosis in cerebral ischemia and traumatic brain injury[82–86] and miR-30e that regulated neuroinflammation in a Parkinson's disease model[87].

Some of the miRNAs that were increased by Enoxacin were reduced in biofluids and tissues from ALS patients or ALS mouse models, suggesting that Enoxacin recovers the expression of these miRNAs. For example, miR-378a levels are reduced in CSF from ALS patients[58] and were increased in the CSF following Enoxacin in our study. miR-320 levels are reduced in the serum or CSF of patients with ALS[47] or FTD [88,89] and in the spinal cord and brainstem of SOD1

G93A mice[90] and are increased in response to Enoxacin therapy.

While the safety profile of Enoxacin is known and this drug has been in clinical use for many years, we also examined for the first time the safety and tolerability of Enoxacin in patients with ALS. At 600mg x2/day one patient dropped out before study completion, due to AEs that were deemed related to the drug, but these AEs were not life-threatening and no other drug-related AEs were observed in other patients.

We did not expect any effect on NfL levels in our trial, as even in the VALOR trial for Tofersen therapy in SOD1-ALS, NFL responded to therapy only after 12 weeks[2]. Therefore, a single month is not expected and is indeed insufficient to demonstrate beneficial effects of Enoxacin on disease trajectory. The single month study encourages a longer study of the efficacy of Enoxacin therapy.

Limitations

The small cohort size hindered the determination of whether the effect of Enoxacin on miRNAs was dose-dependent. The COVID pandemic is the main reason for the relatively low enrolment in 2021 and 2022 and the expiry of the experimental drug batch prevented the extension of the trial further.

Unfortunately, no female patients were enrolled in the study; therefore, we do not know whether there are sex-associated differences in the response to Enoxacin. Finally, the study did not explore efficacy as an endpoint due to the short therapy duration and the small number of patients.

In summary, Enoxacin presents a promising therapeutic option for ALS with an established safety profile, robust mechanistic data, and evidence for target engagement in both human patient plasma and CSF. The ready-to-use pharmacodynamic biomarker package enhances its appeal as a testable compelling addition to the ALS treatment landscape. The recent approval of Tofersen as a therapy for ALS by the FDA, based on its ability to lower blood levels of neurofilament light (NfL)[2] highlights the importance of biomarkers as an endpoint for clinical trials.

Data availability

Data is available upon reasonable request from the author.

Acknowledgements

EH is the Mondry Family Professorial Chair and Head of the Nella and Leon Benoziyo Centre for Neurological Diseases and of the Andi and Larry Wolfe Centre for Neuroimmunology and Neuromodulation. We thank Orla Hardiman (Trinity College Dublin), Dame Pamela Shaw (University of Sheffield), and Leonard van den Berg (University Medical Center Utrecht) for their advice on the study design. We are grateful to Susan Stern, National Executive Director and CEO of Weizmann Canada, and Prof. Erik Storkebaum (Radboud University, Nijmegen) for their involvement. Enoxacin was an in-kind gift from the late Barry Sherman, Alexandra Krawczyk, the Honey & Barry Sherman Legacy Foundation and Apotex Inc., Toronto, Canada. We thank Drs. Brigitte Happ, Kostas Kaloulis, Sonia Poli and Dawn Toronto for their consultation on drug development and regulatory affairs. We thank Yahel Cohen and Dr. Nancy S Yacovzda (WIS) for advice and for comments on the manuscript.

This study was funded by ALS Association clinical trial award (program: 'Repurposing Enoxacin therapy for patients with ALS' 22-CTA-614), ALS Canada-Brain Canada Discovery grant (program: 'Advanced Pharmacokinetics and Pharmacodynamics for phase Ib/IIa trial of repurposed Enoxacin therapy for patients with ALS'), ERA-Net for Research Programs on Rare Diseases (eRARE FP7) via the Israel Ministry of Health and Muscular Dystrophy Canada, Canadian Institutes of Health Research (CIHR) and Fonds de recherche du Québec - Santé (FRQS). IM was supported by Teva Pharmaceutical Industries as part of the Israeli National Network of Excellence in Neuroscience (fellowship no. 117941).

Research at the Hornstein lab is further funded by Andi and Larry Wolfe Centre for Neuroimmunology and Neuromodulation, the Binational Science Foundation (BSF); Association Française Contre les Myopathies (AFM) grants 24882, 28680; Muscular Dystrophy Association (MDA) grant 1280000; Target ALS; Israel Science Foundation (ISF 3497/21, 424/22); ALS Canada; Minna-James-Heineman Stiftung through Minerva, Minerva Foundation, with funding from the Federal German Ministry for Education and Research; Robert Packard Center for ALS Research at Johns Hopkins; McGill University; EU - ERA-Net; Radala Foundation for ALS Research; Additional support generously provided by the Kekst Family Institute for Medical Genetics. Weizmann SABRA - Yeda-Sela - WRC Program, the Estate of Emile Mimran, and The Maurice and Vivienne Wohl Biology Endowment. Nella and Leon Benoziyo Center for Neurological Diseases. Goldhirsh-Yellin Foundation. Dr. Sydney Brenner

and friends. Weizmann - Center for Research on Neurodegeneration. Redhill Foundation – Sam and Jean Rothberg Charitable Trust Dr. Dvora and Haim Teitelbaum Endowment Fund.

The funders were not involved in study design; collection, management, analysis and interpretation of data; or the decision to submit for publication.

Author Contributions

IM, AE, AG and EH contributed to the conception and design of the study; IM, HMK, NP, MM, AG and EH contributed to the acquisition and analysis of data; IM, AG and EH contributed to drafting the text or preparing the figures.

Potential Conflicts of Interest

Nothing to report (for all authors).

REFERENCES

1. Tsai, M.-J., Hsu, C.-Y. & Sheu, C.-C. Amyotrophic Lateral Sclerosis. *N. Engl. J. Med.* **377**, 1602 (2017).
2. Miller, T. M. *et al.* Trial of Antisense Oligonucleotide Tofersen for SOD1 ALS. *N. Engl. J. Med.* **387**, 1099–1110 (2022).
3. Al-Chalabi, A., van den Berg, L. H. & Veldink, J. Gene discovery in amyotrophic lateral sclerosis: implications for clinical management. *Nat. Rev. Neurol.* **13**, 96–104 (2017).
4. Haramati, S. *et al.* miRNA malfunction causes spinal motor neuron disease. *Proc. Natl. Acad. Sci. U. S. A.* **107**, 13111–13116 (2010).
5. Lagier-Tourenne, C., Polymenidou, M. & Cleveland, D. W. TDP-43 and FUS/TLS: emerging roles in RNA processing and neurodegeneration. *Hum. Mol. Genet.* **19**, R46–64 (2010).
6. Lagier-Tourenne, C. & Cleveland, D. W. Rethinking ALS: the FUS about TDP-43. *Cell* **136**, 1001–1004 (2009).
7. Lemmens, R., Moore, M. J., Al-Chalabi, A., Brown, R. H., Jr & Robberecht, W. RNA metabolism and the pathogenesis of motor neuron diseases. *Trends Neurosci.* **33**, 249–258 (2010).
8. Strong, M. J. The evidence for altered RNA metabolism in amyotrophic lateral sclerosis (ALS). *J. Neurol. Sci.* **288**, 1–12 (2010).
9. Irwin, K. E. *et al.* A fluid biomarker reveals loss of TDP-43 splicing repression in presymptomatic ALS-FTD. *Nat. Med.* **30**, 382–393 (2024).
10. Keuss, M. J. *et al.* Loss of TDP-43 induces synaptic dysfunction that is rescued by UNC13A splice-switching ASOs. *bioRxivorg* (2024) doi:10.1101/2024.06.20.599684.
11. Costantino, I., Meng, A. & Ravits, J. Pathologic changes in ELAVL3 expression and splicing occur in TDP43 and non-TDP43 proteinopathies (P4-9.007). *Neurology* **102**, (2024).
12. Cao, M. C. *et al.* A panel of TDP-43-regulated splicing events verifies loss of TDP-43 function in amyotrophic lateral sclerosis brain tissue. *Neurobiol. Dis.* **185**, 106245 (2023).
13. Emde, A. *et al.* Dysregulated miRNA biogenesis downstream of cellular stress and ALS-causing

mutations: a new mechanism for ALS. *EMBO J.* **34**, 2633–2651 (2015).

14. Campos-Melo, D., Droppelmann, C. A., He, Z., Volkening, K. & Strong, M. J. Altered microRNA expression profile in Amyotrophic Lateral Sclerosis: a role in the regulation of NFL mRNA levels. *Mol. Brain* **6**, 26 (2013).
15. Figueroa-Romero, C. *et al.* Expression of microRNAs in human post-mortem amyotrophic lateral sclerosis spinal cords provides insight into disease mechanisms. *Mol. Cell. Neurosci.* **71**, 34–45 (2016).
16. Reichenstein, I. *et al.* Human genetics and neuropathology suggest a link between miR-218 and amyotrophic lateral sclerosis pathophysiology. *Sci. Transl. Med.* **11**, (2019).
17. Kawahara, Y. & Mieda-Sato, A. TDP-43 promotes microRNA biogenesis as a component of the Drosha and Dicer complexes. *Proc. Natl. Acad. Sci. U. S. A.* **109**, 3347–3352 (2012).
18. Bernstein, E., Caudy, A. A., Hammond, S. M. & Hannon, G. J. Role for a bidentate ribonuclease in the initiation step of RNA interference. *Nature* **409**, 363–366 (2001).
19. Yang, J.-S. *et al.* Conserved vertebrate mir-451 provides a platform for Dicer-independent, Ago2-mediated microRNA biogenesis. *Proc. Natl. Acad. Sci. U. S. A.* **107**, 15163–15168 (2010).
20. Kretov, D. A. *et al.* Ago2-Dependent Processing Allows miR-451 to Evade the Global MicroRNA Turnover Elicited during Erythropoiesis. *Mol. Cell* **78**, 317–328.e6 (2020).
21. Melo, S. *et al.* Small molecule enoxacin is a cancer-specific growth inhibitor that acts by enhancing TAR RNA-binding protein 2-mediated microRNA processing. *Proc. Natl. Acad. Sci. U. S. A.* **108**, 4394–4399 (2011).
22. Schaeffer, A. J. The expanding role of fluoroquinolones. *Am. J. Med.* **113 Suppl 1A**, 45S–54S (2002).
23. Shan, G. *et al.* A small molecule enhances RNA interference and promotes microRNA processing. *Nat. Biotechnol.* **26**, 933–940 (2008).
24. Smalheiser, N. R., Zhang, H. & Dwivedi, Y. Enoxacin Elevates MicroRNA Levels in Rat Frontal Cortex and Prevents Learned Helplessness. *Front. Psychiatry* **5**, 6 (2014).
25. Rizzuti, M. *et al.* MicroRNA expression analysis identifies a subset of downregulated miRNAs in ALS motor neuron progenitors. *Sci. Rep.* **8**, 10105 (2018).
26. Shelkovnikova, T. A. *et al.* Protective paraspeckle hyper-assembly downstream of TDP-43 loss of function in amyotrophic lateral sclerosis. *Mol. Neurodegener.* **13**, (2018).

27. Arakawa, Y. *et al.* Association between oxidative stress and microRNA expression pattern of ALS patients in the high-incidence area of the Kii Peninsula. *Brain Res.* **1746**, 147035 (2020).
28. Banack, S. A., Dunlop, R. A. & Cox, P. A. An miRNA fingerprint using neural-enriched extracellular vesicles from blood plasma: towards a biomarker for amyotrophic lateral sclerosis/motor neuron disease. *Open Biol.* **10**, 200116 (2020).
29. Benigni, M. *et al.* Identification of miRNAs as Potential Biomarkers in Cerebrospinal Fluid from Amyotrophic Lateral Sclerosis Patients. *Neuromolecular Med.* **18**, 551–560 (2016).
30. Cloutier, F., Marrero, A., O'Connell, C. & Morin, P., Jr. MicroRNAs as potential circulating biomarkers for amyotrophic lateral sclerosis. *J. Mol. Neurosci.* **56**, 102–112 (2015).
31. Daneshafrooz, N. *et al.* Identification of let-7f and miR-338 as plasma-based biomarkers for sporadic amyotrophic lateral sclerosis using meta-analysis and empirical validation. *Sci. Rep.* **12**, 1373 (2022).
32. de Andrade, H. M. T. *et al.* MicroRNAs-424 and 206 are potential prognostic markers in spinal onset amyotrophic lateral sclerosis. *J. Neurol. Sci.* **368**, 19–24 (2016).
33. De Felice, B. *et al.* miR-338-3p is over-expressed in blood, CFS, serum and spinal cord from sporadic amyotrophic lateral sclerosis patients. *Neurogenetics* **15**, 243–253 (2014).
34. De Luna, N. *et al.* Downregulation of miR-335-5P in Amyotrophic Lateral Sclerosis Can Contribute to Neuronal Mitochondrial Dysfunction and Apoptosis. *Sci. Rep.* **10**, 4308 (2020).
35. Dobrowolny, G. *et al.* A longitudinal study defined circulating microRNAs as reliable biomarkers for disease prognosis and progression in ALS human patients. *Cell Death Discov* **7**, 4 (2021).
36. Freischmidt, A. *et al.* Serum microRNAs in sporadic amyotrophic lateral sclerosis. *Neurobiol. Aging* **36**, 2660.e15–20 (2015).
37. Giagnorio, E. *et al.* MiR-146a in ALS: Contribution to Early Peripheral Nerve Degeneration and Relevance as Disease Biomarker. *Int. J. Mol. Sci.* **24**, (2023).
38. Joilin, G., Leigh, P. N., Newbury, S. F. & Hafezparast, M. An Overview of MicroRNAs as Biomarkers of ALS. *Front. Neurol.* **10**, 186 (2019).
39. Joilin, G. *et al.* Identification of a potential non-coding RNA biomarker signature for amyotrophic lateral sclerosis. *Brain Commun* **2**, fcaa053 (2020).
40. Katsu, M. *et al.* MicroRNA expression profiles of neuron-derived extracellular vesicles in plasma from patients with amyotrophic lateral sclerosis. *Neurosci. Lett.* **708**, 134176 (2019).

41. Liguori, M. *et al.* Dysregulation of MicroRNAs and Target Genes Networks in Peripheral Blood of Patients With Sporadic Amyotrophic Lateral Sclerosis. *Front. Mol. Neurosci.* **11**, 288 (2018).
42. Lo, T.-W. *et al.* Extracellular Vesicles in Serum and Central Nervous System Tissues Contain microRNA Signatures in Sporadic Amyotrophic Lateral Sclerosis. *Front. Mol. Neurosci.* **14**, 739016 (2021).
43. Malacarne, C. *et al.* Dysregulation of Muscle-Specific MicroRNAs as Common Pathogenic Feature Associated with Muscle Atrophy in ALS, SMA and SBMA: Evidence from Animal Models and Human Patients. *Int. J. Mol. Sci.* **22**, (2021).
44. Matamala, J. M. *et al.* Genome-wide circulating microRNA expression profiling reveals potential biomarkers for amyotrophic lateral sclerosis. *Neurobiol. Aging* **64**, 123–138 (2018).
45. Panio, A., Cava, C., D'Antona, S., Bertoli, G. & Porro, D. Diagnostic Circulating miRNAs in Sporadic Amyotrophic Lateral Sclerosis. *Front. Med.* **9**, 861960 (2022).
46. Pregnolato, F. *et al.* Exosome microRNAs in Amyotrophic Lateral Sclerosis: A Pilot Study. *Biomolecules* **11**, (2021).
47. Raheja, R. *et al.* Correlating serum micrornas and clinical parameters in amyotrophic lateral sclerosis. *Muscle Nerve* **58**, 261–269 (2018).
48. Ravnik-Glavač, M. & Glavač, D. Circulating RNAs as Potential Biomarkers in Amyotrophic Lateral Sclerosis. *Int. J. Mol. Sci.* **21**, (2020).
49. Ricci, C., Marzocchi, C. & Battistini, S. MicroRNAs as Biomarkers in Amyotrophic Lateral Sclerosis. *Cells* **7**, (2018).
50. Saucier, D. *et al.* Identification of a circulating miRNA signature in extracellular vesicles collected from amyotrophic lateral sclerosis patients. *Brain Res.* **1708**, 100–108 (2019).
51. Sheinerman, K. S. *et al.* Circulating brain-enriched microRNAs as novel biomarkers for detection and differentiation of neurodegenerative diseases. *Alzheimers. Res. Ther.* **9**, 89 (2017).
52. Soliman, R. *et al.* Assessment of diagnostic potential of some circulating microRNAs in Amyotrophic Lateral Sclerosis Patients, an Egyptian study. *Clin. Neurol. Neurosurg.* **208**, 106883 (2021).
53. Sproviero, D. *et al.* Different miRNA Profiles in Plasma Derived Small and Large Extracellular Vesicles from Patients with Neurodegenerative Diseases. *Int. J. Mol. Sci.* **22**, (2021).

54. Takahashi, I. *et al.* Identification of plasma microRNAs as a biomarker of sporadic Amyotrophic Lateral Sclerosis. *Mol. Brain* **8**, 67 (2015).

55. Tasca, E., Pegoraro, V., Merico, A. & Angelini, C. Circulating microRNAs as biomarkers of muscle differentiation and atrophy in ALS. *Clin. Neuropathol.* **35**, 22–30 (2016).

56. Toivonen, J. M. *et al.* MicroRNA-206: a potential circulating biomarker candidate for amyotrophic lateral sclerosis. *PLoS One* **9**, e89065 (2014).

57. Waller, R. *et al.* Serum miRNAs miR-206, 143-3p and 374b-5p as potential biomarkers for amyotrophic lateral sclerosis (ALS). *Neurobiol. Aging* **55**, 123–131 (2017).

58. Waller, R. *et al.* Small RNA Sequencing of Sporadic Amyotrophic Lateral Sclerosis Cerebrospinal Fluid Reveals Differentially Expressed miRNAs Related to Neural and Glial Activity. *Front. Neurosci.* **11**, 731 (2017).

59. Benatar, M. *et al.* Prognostic clinical and biological markers for amyotrophic lateral sclerosis disease progression: validation and implications for clinical trial design and analysis. *EBioMedicine* **108**, 105323 (2024).

60. Magen, I. *et al.* Circulating miR-181 is a prognostic biomarker for amyotrophic lateral sclerosis. *Nat. Neurosci.* **24**, 1534–1541 (2021).

61. Magen, I. *et al.* Muscle microRNAs in the cerebrospinal fluid predict clinical response to nusinersen therapy in type II and type III spinal muscular atrophy patients. *Eur. J. Neurol.* **29**, 2420–2430 (2022).

62. Magen, I. *et al.* microRNA-based predictor for diagnosis of frontotemporal dementia. *Neuropathol. Appl. Neurobiol.* **49**, e12916 (2023).

63. Scholar, E. Enoxacin. in *xPharm: The Comprehensive Pharmacology Reference* 1–6 (Elsevier, 2007).

64. Enoxacin Dosage. *Drugs.com* https://www.drugs.com/dosage/enoxacin.html.

65. Sanderink, G. J., Bournique, B., Stevens, J., Petry, M. & Martinet, M. Involvement of human CYP1A isoenzymes in the metabolism and drug interactions of riluzole in vitro. *J. Pharmacol. Exp. Ther.* **282**, 1465–1472 (1997).

66. Coenen-Stass, A. M. L. *et al.* Evaluation of methodologies for microRNA biomarker detection by next generation sequencing. *RNA Biol.* **15**, 1133–1145 (2018).

67. Kozomara, A. & Griffiths-Jones, S. miRBase: annotating high confidence microRNAs using

deep sequencing data. *Nucleic Acids Res.* **42**, D68–73 (2014).

68. Love, M. I., Huber, W. & Anders, S. Moderated estimation of fold change and dispersion for RNA-seq data with DESeq2. *Genome Biol.* **15**, 550 (2014).
69. Benjamini, Y., Drai, D., Elmer, G., Kafkafi, N. & Golani, I. Controlling the false discovery rate in behavior genetics research. *Behav. Brain Res.* **125**, 279–284 (2001).
70. Benjamini, Y., Krieger, A. M. & Yekutieli, D. Adaptive linear step-up procedures that control the false discovery rate. *Biometrika* **93**, 491–507 (2006).
71. Le Liboux, A. *et al.* Single- and multiple-dose pharmacokinetics of riluzole in white subjects. *J. Clin. Pharmacol.* **37**, 820–827 (1997).
72. Wymer, J., Apple, S., Harrison, A. & Hill, B. A. Pharmacokinetics, Bioavailability, and Swallowing Safety With Riluzole Oral Film. *Clin Pharmacol Drug Dev* **12**, 57–64 (2023).
73. Tran Van Tho, Armengaud, A. & Davet, B. Diffusion of enoxacin into the cerebrospinal fluid in dogs with healthy meninges and with experimental meningitis. *J. Antimicrob. Chemother.* **14 Suppl C**, 57–62 (1984).
74. Delon, A. *et al.* Pharmacokinetic-pharmacodynamic contributions to the convulsant activity of fluoroquinolones in rats. *Antimicrob. Agents Chemother.* **43**, 1511–1515 (1999).
75. Marchand, S., Pariat, C., Boulanger, A., Bouquet, S. & Couet, W. A pharmacokinetic/pharmacodynamic approach to show that not all fluoroquinolones exhibit similar sensitivity toward the proconvulsant effect of biphenyl acetic acid in rats. *J. Antimicrob. Chemother.* **48**, 813–820 (2001).
76. Kawakami, J., Ohashi, K., Yamamoto, K., Sawada, Y. & Iga, T. Effect of acute renal failure on neurotoxicity of enoxacin in rats. *Biol. Pharm. Bull.* **20**, 931–934 (1997).
77. Keller, A. *et al.* miRNATissueAtlas2: an update to the human miRNA tissue atlas. *Nucleic Acids Res.* **50**, D211–D221 (2022).
78. Hawkins, S. *et al.* Upregulation of β-catenin due to loss of miR-139 contributes to motor neuron death in amyotrophic lateral sclerosis. *Stem Cell Reports* **17**, 1650–1665 (2022).
79. Wang, Y. *et al.* miR-130a alleviates neuronal apoptosis and changes in expression of Bcl-2/Bax and caspase-3 in cerebral infarction rats through PTEN/PI3K/Akt signaling pathway. *Exp. Ther. Med.* **19**, 2119–2126 (2020).
80. Zhang, C.-Y. *et al.* Effect of miR-130a on neuronal injury in rats with intracranial hemorrhage

through PTEN/PI3K/AKT signaling pathway. *Eur. Rev. Med. Pharmacol. Sci.* **23**, 4890–4897 (2019).

81. Zheng, T. *et al.* MiR-130a exerts neuroprotective effects against ischemic stroke through PTEN/PI3K/AKT pathway. *Biomed. Pharmacother.* **117**, 109117 (2019).
82. Ma, Q. *et al.* Blood microRNA-93 as an indicator for diagnosis and prediction of functional recovery of acute stroke patients. *J. Clin. Neurosci.* **62**, 121–127 (2019).
83. Ni, J. *et al.* MicroRNA let-7c-5p protects against cerebral ischemia injury via mechanisms involving the inhibition of microglia activation. *Brain Behav. Immun.* **49**, 75–85 (2015).
84. Tian, F., Yuan, C., Hu, L. & Shan, S. MicroRNA-93 inhibits inflammatory responses and cell apoptosis after cerebral ischemia reperfusion by targeting interleukin-1 receptor-associated kinase 4. *Exp. Ther. Med.* **14**, 2903–2910 (2017).
85. Zhang, N. *et al.* MicroRNA-378 Alleviates Cerebral Ischemic Injury by Negatively Regulating Apoptosis Executioner Caspase-3. *Int. J. Mol. Sci.* **17**, (2016).
86. Zhu, G. *et al.* MSCs-derived exosomes containing miR-486-5p attenuate cerebral ischemia and reperfusion (I/R) injury. *Gene* **906**, 148262 (2024).
87. Li, D. *et al.* MicroRNA-30e regulates neuroinflammation in MPTP model of Parkinson's disease by targeting Nlrp3. *Hum. Cell* **31**, 106–115 (2018).
88. Denk, J. *et al.* Specific serum and CSF microRNA profiles distinguish sporadic behavioural variant of frontotemporal dementia compared with Alzheimer patients and cognitively healthy controls. *PLoS One* **13**, e0197329 (2018).
89. Tan, Y. J. *et al.* Altered Cerebrospinal Fluid Exosomal microRNA Levels in Young-Onset Alzheimer's Disease and Frontotemporal Dementia. *J Alzheimers Dis Rep* **5**, 805–813 (2021).
90. Zhou, F. *et al.* Screening the expression characteristics of several miRNAs in G93A-SOD1 transgenic mouse: altered expression of miRNA-124 is associated with astrocyte differentiation by targeting Sox2 and Sox9. *J. Neurochem.* **145**, 51–67 (2018).

MAIN TABLES

Characteristic	200mg x 2/day (N=3)	400mg x 2/day (N=3)	600mg x 2/day (N=2)	Total (N=8)
Sex, male	3 (100%)	3 (100%)	2 (100%)	8 (100%)
Age, years	67 (6.6), 60-73	60.3 (6.8), 55-68	69.5 (2.1), 68-71	65.1 (6.6), 55-73

Height, cm	179 (7.5), 171-185	163 (9.8), 152-172	174 (8.7), 168-180	172 (11.7), 152-185
Weight kg	73 (11), 62-84	83.9 (17.2), 66-100	78.8 (3.4), 76.4-81.2	78.6 (12.1), 62-100
Symptom duration, months	19.1 (6.5), 11.6-23.3	34.9 (33.4), 10.3-72.9	11 (0.4), 10.7-11.3	23 (21), 10.3–72.9
Diagnostic delay, months	11.3 (9.1), 8.3 – 19.3	14.5 (18.6), 2.9 - 36	9.4 (1.2), 8.5 – 10.3	12.2 (8.9), 2.9 - 36
El Escorial, definite	1 (33%)	1 (33%)	0	2 (25%)
Site of onset, bulbar	0	1 (33%)	2 (100%)	3 (38%)
Concomitant ALS medication use				
Riluzole only	2 (67%)	2 (67%)	2 (100%)	6 (75%)
Riluzole and Edaravone	1 (33%)	1 (33%)	0	2 (25%)
ALSFRS-R total score	31.3 (6.4), 24-36	32.3 (4.7), 27-36	38.5 (4.9), 35-42	33.5 (5.6), 24-42
ΔFRS, points per months	-1.1 (0.86), -2.1 – (0.54)	-0.95 (0.97), -2 – (-0.16)	-0.86 (0.42), -1.15 – (-0.56)	-0.97 (0.72), -2.1 – (-0.16)
FVC, % predicted	82.6 (27.2), 51.7-103	82.6 (17.6), 64-98.9	58 (1.4), 57-59	76.5 (20.8), 51.7-103
King's stage 2/3/4 (N)	1/1/1	1/1/1	0/1/1	2/3/3

Table 1. Characteristics of patients at baseline. Continuous data are presented with mean (standard deviation) and range, categorical data are presented as frequency (percentage).

ΔFRS = (48-ALSFRS-R total score)/ symptom duration.

SUPPLEMENTARY TABLES

Enoxacin pharmacokinetics

C_{trough} (ng/ml)				C_{max} (ng/ml)		t_{max} (hr)	
Day 7	**Day 14**	**Day 21**	**Day 30**	**Day 1**	**Day 30**	**Day 1**	**Day 30**
628	563	548	685	1324	1752	2	2 (1)

(286)	(250)	(288)	(296)	(477)	(475)	(1.1)

Supplementary table 1. Pharmacokinetic parameters of Enoxacin in plasma: trough concentrations on days 7, 14, 21 and 30 before morning dose, maximal concentrations and time to reach maximal concentrations on days 1 and 30 after Enoxacin morning dose. Data are presented as mean (sd).

Riluzole concentration (ng/ml)							
Day 1				**Day 30**			
2h	**4h**	**6h**	**8h**	**2h**	**4h**	**6h**	**8h**
93.53 (35.7)	82.4 (31.7)	78.0 (36.7)	66.67 (34.1)	237.3** (84.4)	209.3* (96.7)	177.8* (99.1)	156.7* (90.6)

Supplementary table 2. Plasma Riluzole concentrations on days 1 and 30 at the indicated times after Enoxacin morning dose. Data presented as mean (sd). *FDR<0.05, **FDR<0.01 compared to the respective hour on day 1, repeated measure ANOVA followed by Benjamini-Hochberg correction.

Dosing group	**200mg x 2/day (N=3)**		**400mg x 2/day (N=3)**		**600mg x 2/day (N=2)**	
Adverse event	**No of patients (%)**	**No of times reported**	**No of patients (%)**	**No of times reported**	**No of patients (%)**	**No of times reported**
Any adverse event	3 (100%)	13	3 (100%)	27	2 (100%)	12
Serious adverse event	0	0	0	0	0	0
Adverse event leading to discontinuation	0	0	0	0	1 (50%)	2

Severity						
Mild	2 (67%)	10	3 (100%)	16	2 (100%)	10
Moderate	1 (33%)	1	2 (67%)	10	1 (50%)	2
Severe	2 (67%)	2	1 (33%)	1	0	0
System organ class						
Nervous system	1 (33%)	1	2 (67%)	12	1 (50%)	3
Gastrointestinal	2 (67%)	6	2 (67%)	2	2 (100%)	8
Musculoskeletal	1 (33%)	2	2 (67%)	5		
Injury, poisoning and procedural complications	2 (67%)	2	1 (33%)	2		
General system disorders			2 (67%)	3	1 (50%)	1
Respiratory			1 (33%)	1		
Psychiatric			1 (33%)	2		
Vascular	1 (33%)	1				
Appetite	1 (33%)	1				
Related to drug	1 (33%)	5	2 (67%)	7	1 (50%)	7
System organ class						
Gastrointestinal						
Nausea	1 (33%)	4			1 (50%)*	3
Nervous system disorder						
Dizziness			1 (33%)	4	1 (50%)*	3
Headache			1 (33%)	2		
General system disorders						
Fatigue			1 (33%)	1		
Excess sweating					1 (50%)	1
Appetite						
Decreased appetite	1 (33%)	1				

Supplementary table 3. Overview of adverse events in patients with ALS treated with Enoxacin.
*Increase in the severity of these AEs caused early termination.

MAIN FIGURES

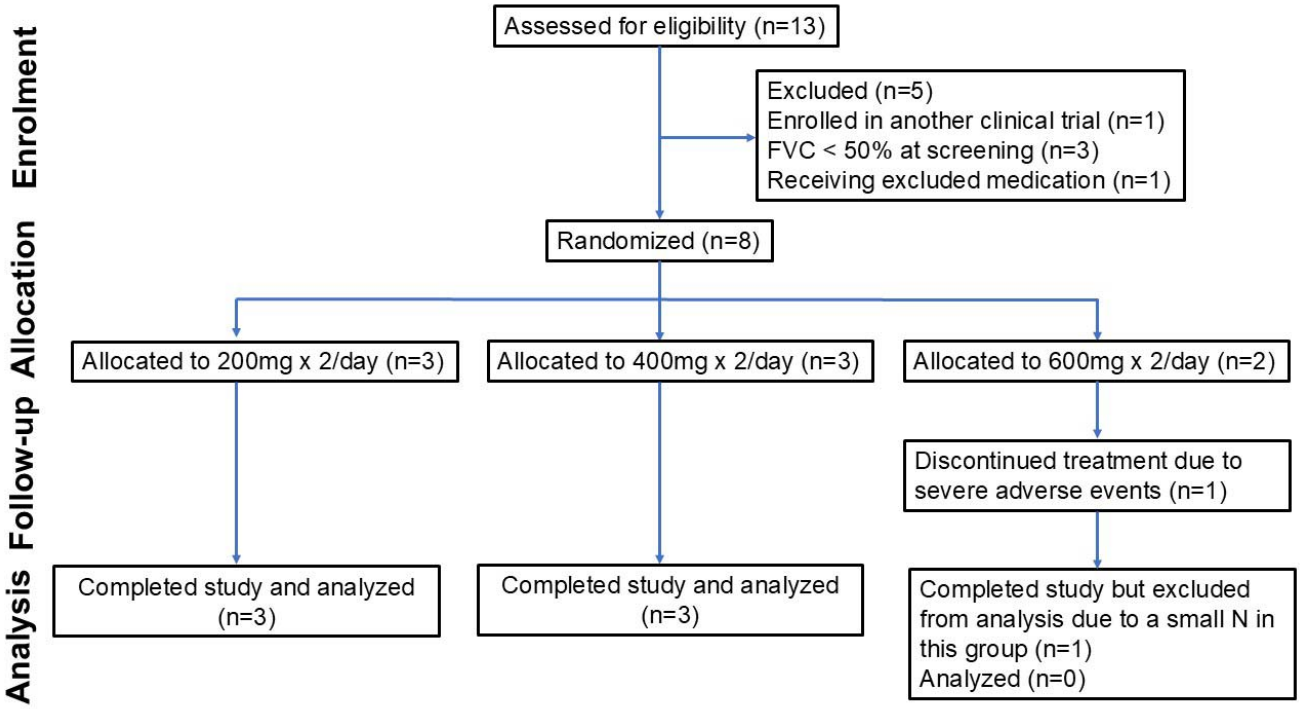

Figure 1. CONSORT flow diagram of the REALS1 trial.

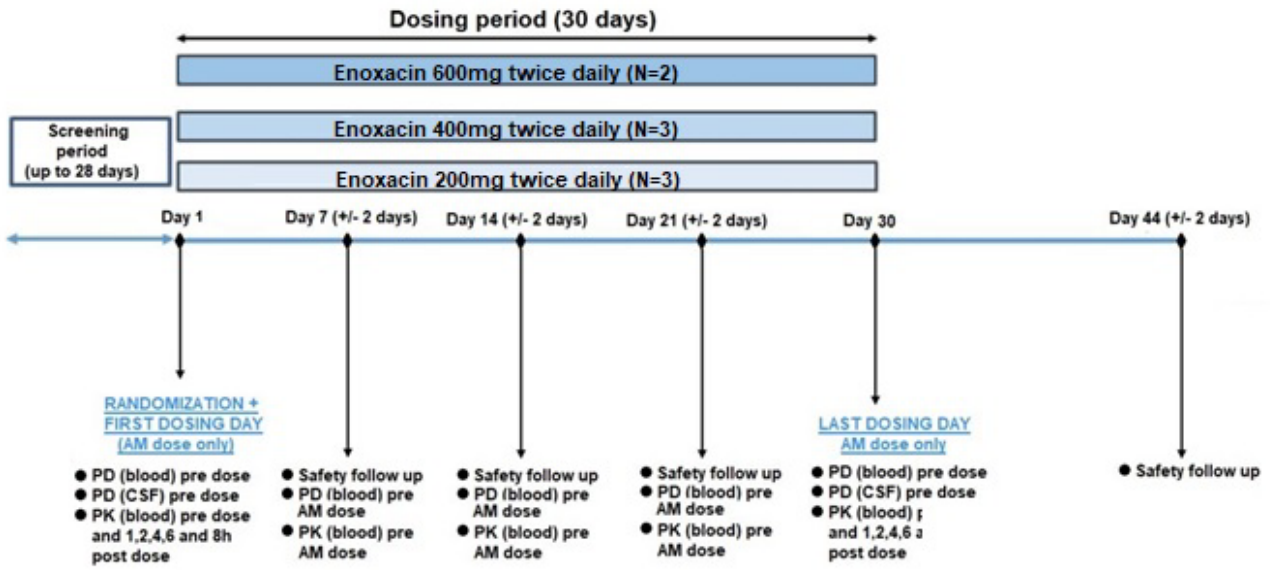

Figure 2. Illustration of study design. Dosing was performed over 30 days with 14 days follow up for reporting adverse effects. Blood and CSF were collected pre-dosing (day 1). CSF was collected again on day 30. Blood was withdrawn on days 7, 14, 21 and 30 with -/+ 2 days variation.

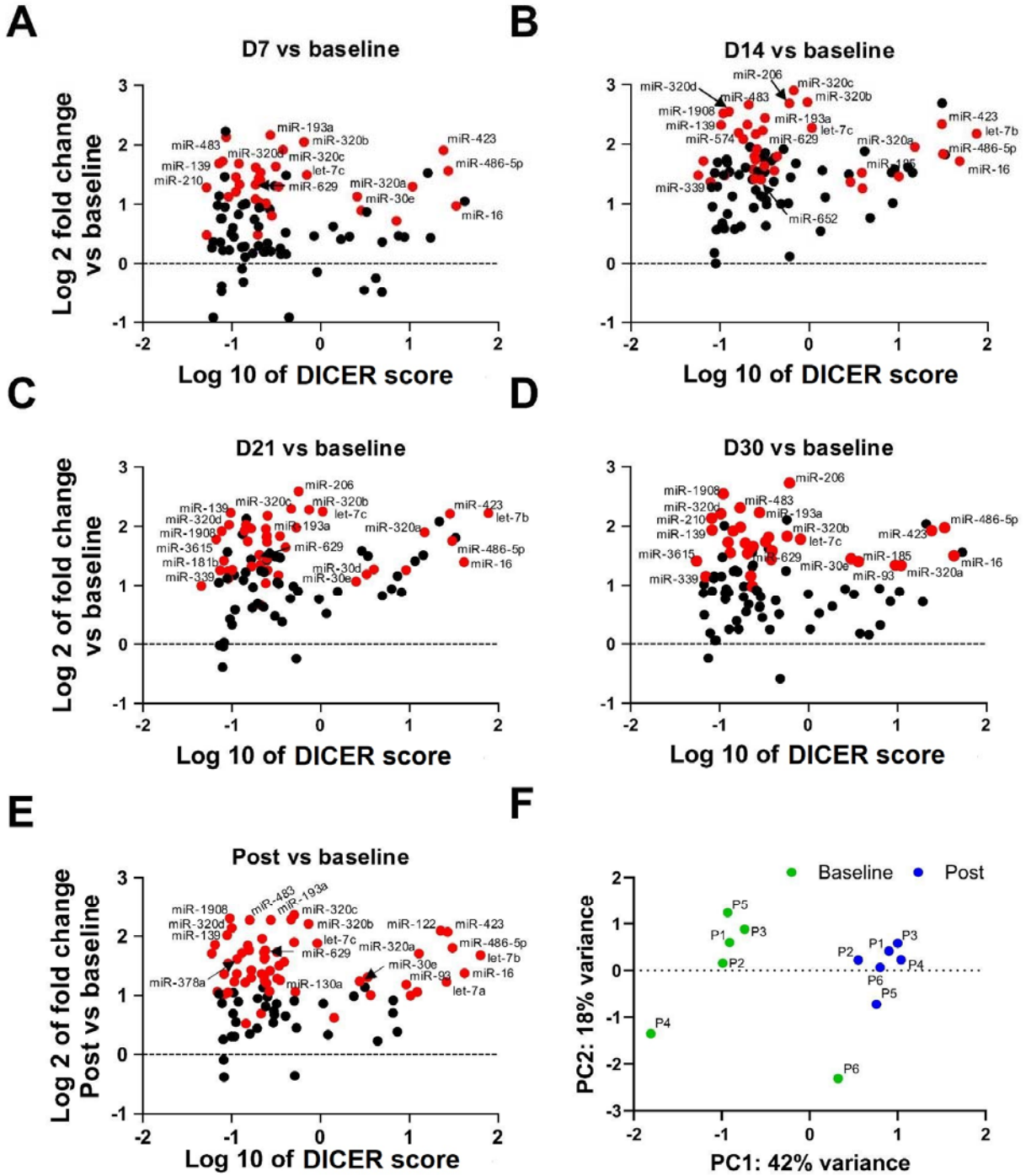

Figure 3. Change in specific miRNA levels in the plasma, compared to baseline levels, on days 7 **(A)**, 14 **(B)**, 21 **(C)**, 30 **(D)** and in all four time points averaged, compared to baseline **(E)**. miRNA counts were corrected to patients and divided by miR-451a levels to generate a "DICER score". Log 2 transformed fold change (y-axis) is shown against Log 10 transformed DICER scores (x-axis). Red indicates miRNAs which are significantly changed vs baseline (FDR<0.1 after multiple hypotheses correction). **(F)** principal component analysis of data presented in E by individual patients. Dots are annotated with the patient number. Green/blue dots denote baseline/post-treatment samples. Data in panels A-D were analyzed with two-way repeated measure ANOVA, data in E were analyzed with multiple t-tests. Multiple hypothesis correction was performed by a Two-stage linear step-up procedure of Benjamini, Krieger and Yekutieli.

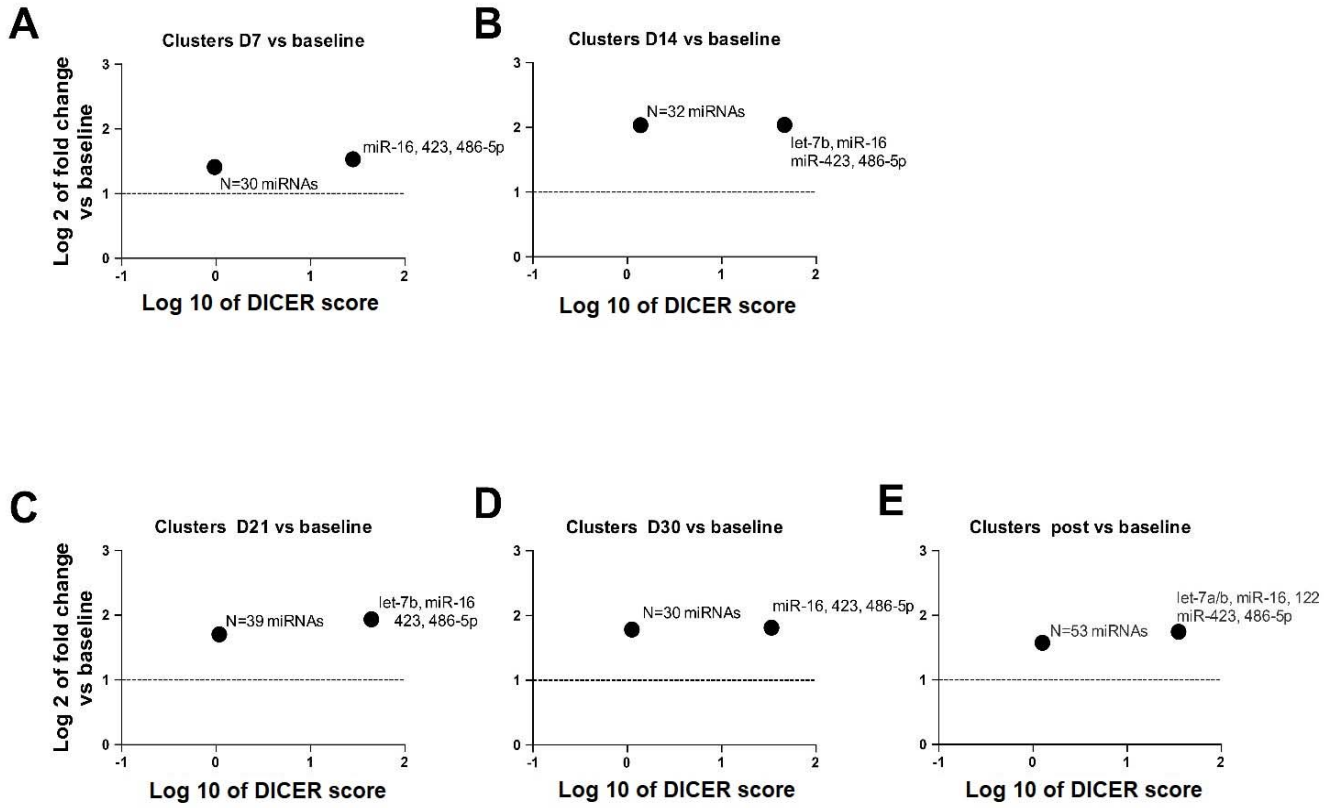

Figure 4. Centroids of k-mean clustering of changes in specific miRNA levels in the plasma, compared to baseline levels, on days 7 **(A)**, 14 **(B)**, 21 **(C)**, 30 **(D)** and in all four time points averaged, compared to baseline **(E)**. miRNA counts were corrected to patients and divided by miR-451a levels. K-mean clustering was performed for the significantly increased miRNAs, with k=2 clusters. Log 2 transformed fold change (y-axis) is shown against Log 10 transformed DICER score (x-axis). Next to each centroid are annotations, or number of the miRNAs included in the corresponding cluster.

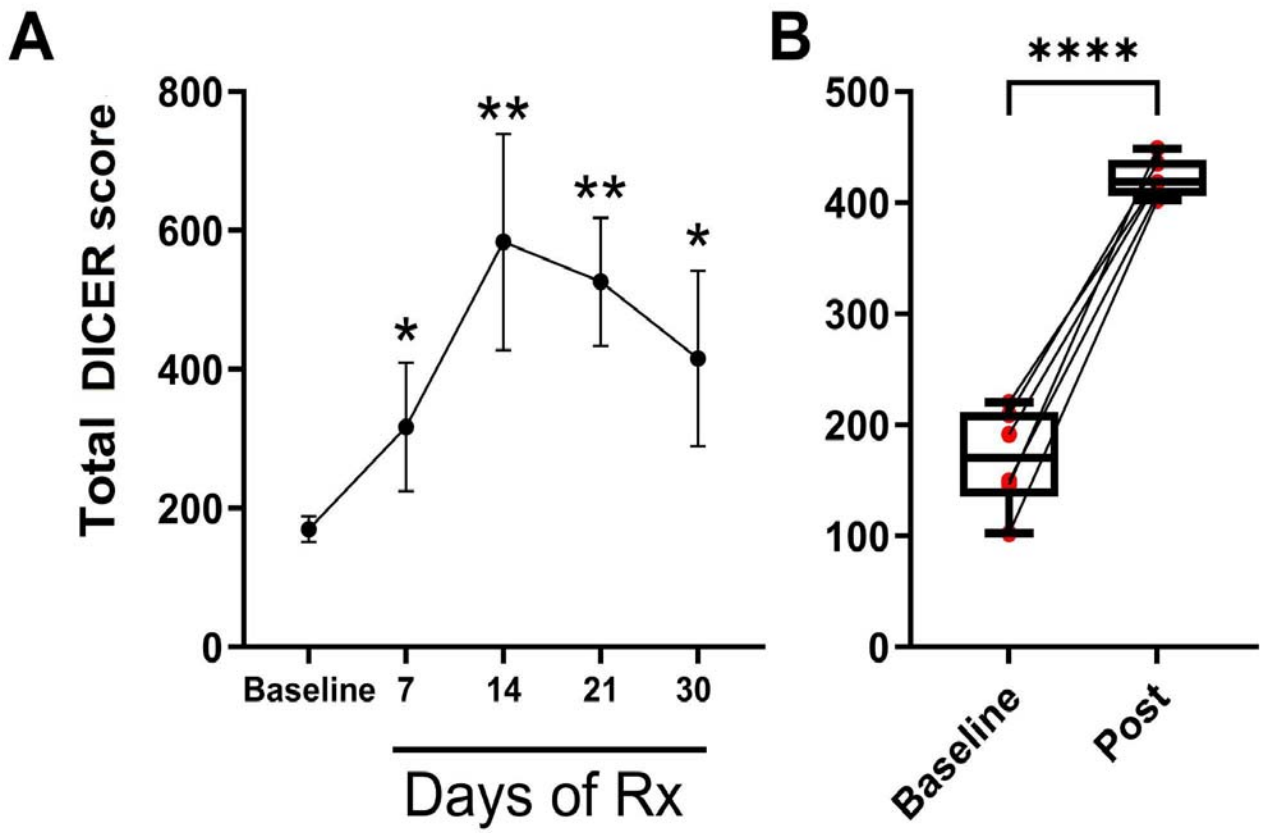

Figure 5. (A) Total DICER score in the plasma at baseline and on days 7, 14, 21 and 30 before morning dose (N=6 patients per time point). *FDR<0.1, **FDR<0.01 for comparisons vs baseline, Friedman test followed by Benjamini-Hochberg correction. **(B)** Total DICER score in the plasma at baseline and post treatment (average of days 7, 14, 21 and 30). ***p<0.0001 vs baseline, paired t-test.

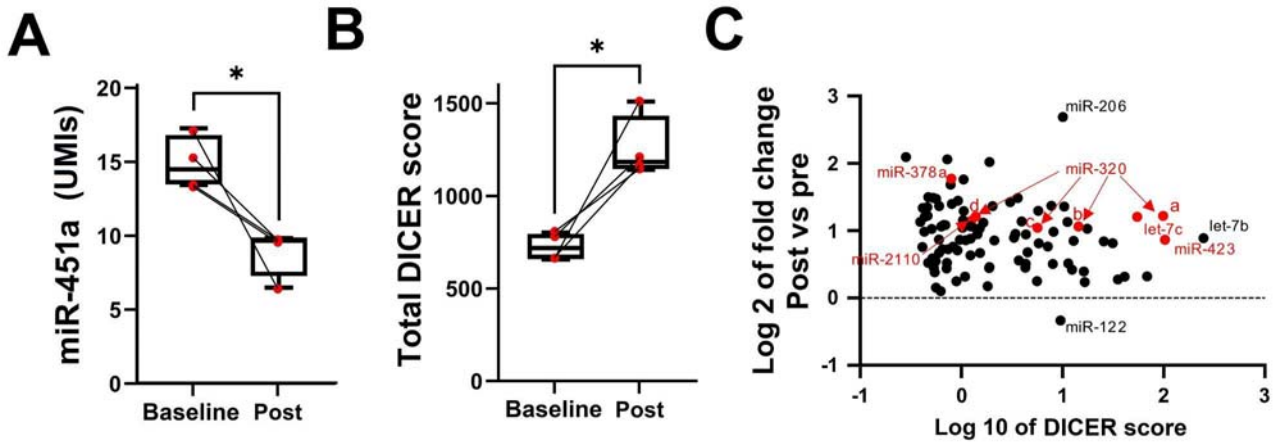

Figure 6. (A) CSF miR-451a decreases after Enoxacin treatment **(B)** Total DICER score in the CSF at baseline and at the completion of 1-month treatment with Enoxacin. *p<0.05, paired t-test. Data are presented as the mean ± SEM of four patients per time point. **(C)** change in specific DICER scores after 1-month treatment compared to baseline levels. miRNA counts in each sample were corrected to patients and divided by the corresponding levels of miR-451a. Log 2 transformed fold change (y-axis) is shown against log 10 transformed of DICER scores (x-axis). Red indicates significantly changed miRNAs (FDR < 0.1, multiple paired t-test followed by the two-stage linear step-up procedure of Benjamini, Krieger and Yekutieli). miR-320 family members are shown with their suffix letter (a, b, c, d) next to the data point.

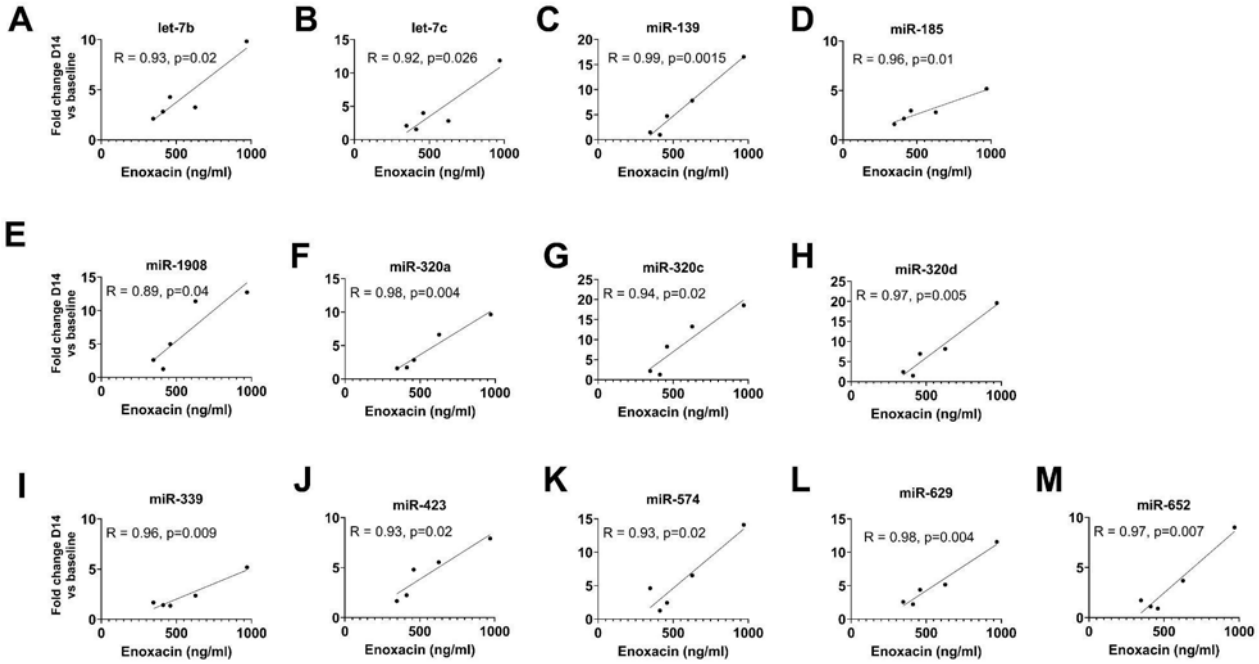

Figure 7. Pearson correlation between Enoxacin levels and fold-change values of miRNAs measured on day 14. p-values shown are unadjusted. All p-values displayed an FDR<0.1 after Benjamini-Hochberg correction.

SUPPLEMENTARY FIGURES

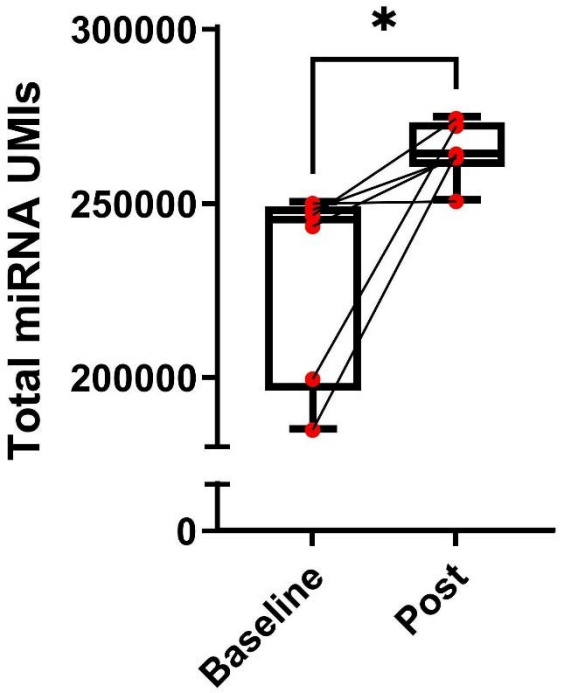

Supplementary figure 1. Total miRNA levels in the plasma, normalized by DESeq2, at baseline and post treatment (average of days 7, 14, 21 and 30). *p<0.05 vs baseline, paired t-test.

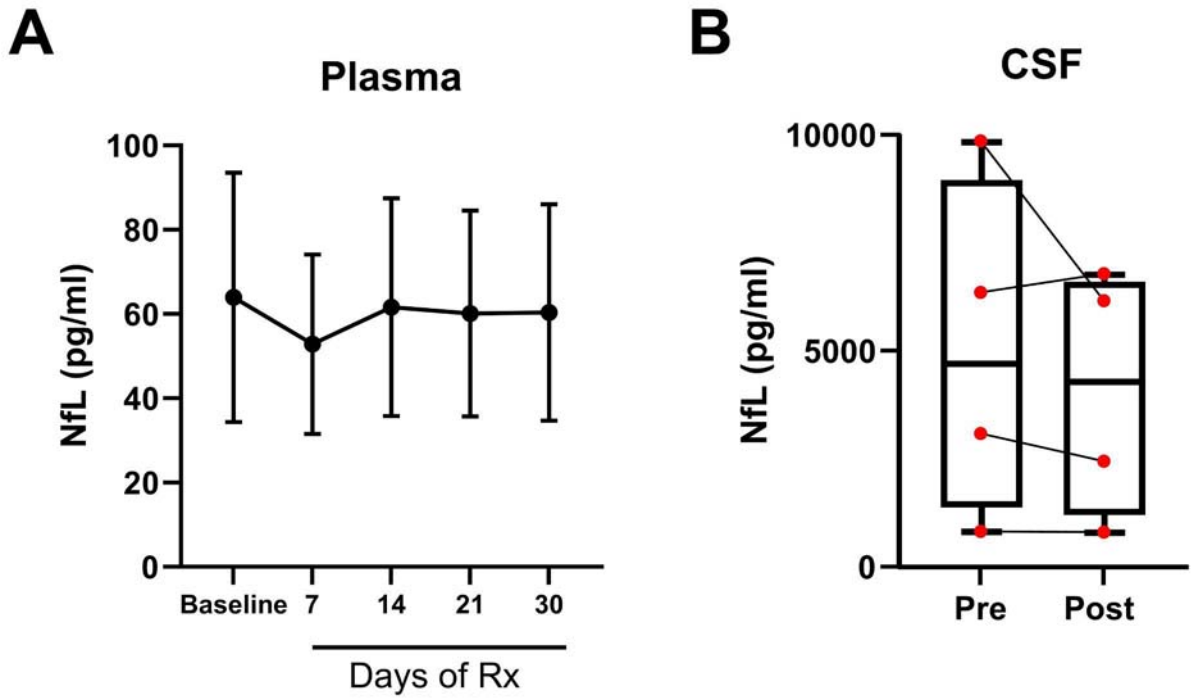

Supplementary figure 2. NfL levels measured in plasma **(A)** and CSF **(B)**. Enoxacin did not affect NfL levels in plasma (one-way repeated measure ANOVA: p=0.27), or in the CSF (p=0.37, paired sample t-test).